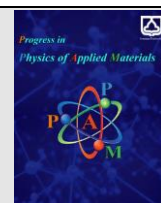




Semnan University

Progress in Physics of Applied Materials

journal homepage: <https://ppam.semnan.ac.ir/>

Morphological and multifractal studies of nanocrystalline Au films

Mehrdad Ahmadi, Maryam Nasehnejad*

Technical and Vocational University (TVU), Department of physics, 1435761137, Tehran, Iran

ARTICLE INFO

Article history:

Received: 28 January 2024

Revised: 28 February 2024

Accepted: 2 March 2024

Keywords:

Surface roughness

Atomic force microscopy (AFM)

Electrodeposition

Multifractal analysis

Au films

ABSTRACT

In this study, we investigated the surface morphology of Au coatings using atomic force microscopy (AFM). We aimed to understand the growth mechanisms and control the nano- and micro-structure of the films to achieve desired morphological properties. The study focused on films formed by the electrodeposition technique and examined the morphology evolution as a function of film thickness. To verify the crystalline structure of the films, X-ray diffraction (XRD) technique was employed. Statistical tests were conducted to confirm that the gold thin film surfaces under investigation exhibited multifractal properties. It is found that as the film thickness increased, the multifractality of the films became more pronounced, and the nonuniformity of the height probabilities also increased. Furthermore, it was observed that surfaces with greater roughness displayed larger nonlinearity and wider width of the multifractal spectrum. The results indicated that the multifractal spectrum had a right-hook shape, distinguishing between different film thicknesses even in small sizes of hundreds of nanometers. Overall, this study provides important insights into the surface morphology of Au coatings and highlights the significance of controlling growth mechanisms for fabricating flat Au films with desired morphological properties. These findings have implications for various applications in biological, electronic, and optical devices.

1. Introduction

Numerous research studies have indicated that when at least one dimension of a material is confined to less than 100 nm, such as in nano-materials, the mechanical, thermal, electrical, and optical properties can undergo significant changes.

Consequently, the same material exhibits distinct characteristics compared to its bulk form. Nowadays, nanostructured thin films play a crucial role in various fields of material science and technology applications. The growth of thin films under non-equilibrium conditions is a complex and random process. By studying the morphologies of growing surfaces and their impact on physical and structural properties, we can gain insights into these processes and fabricate films with desired attributes [1].

Micro-electro-mechanical system (MEMS) find wide applications in automotive vehicles, chemical analysis, medical devices, mobile phones, and wearable equipment.

The fundamental mechanical structures for MEMS sensors and actuators are micro-scale cantilevers and supported beams. Fabricating these three-dimensional micro-structures is a complex process involving photolithography, deposition, and sacrifice etching. Silicon and glass are commonly used as substrate materials for this purpose. Gold is an ideal material for MEMS due to its high inertness, electrical conductivity, low hardness, and resistance to oxidation at room temperature [2]. Gold is a solid transition metal under standard conditions and is known for its attractive luster and resistance to tarnishing in air or water. In the microcantilever sensor community, gold films are extensively used to attach organic functionalized molecules, such as modified alkanethiols, onto silicon cantilevers [3]. These gold films exhibit spectral absorptivity across visible to far infrared radiations and have been employed as infrared absorber coatings in uncooled infrared detectors [4]. In addition, Au thin film has found extensive use as an electrode in the ethanol oxidation

* Corresponding author.

E-mail address: m.nasehnejad@gmail.com

Cite this article as:

Ahmadi M., Nasehnejad M., 2024. Morphological and multifractal study of nanocrystalline Au films. *Progress in Physics of Applied Materials*, 4(1), pp.27-35. DOI: [10.22075/PPAM.2024.32997.1084](https://doi.org/10.22075/PPAM.2024.32997.1084)

© 2024 The Author(s). Journal of Progress in Physics of Applied Materials published by Semnan University Press. This is an open access article under the CC-BY 4.0 license. (<https://creativecommons.org/licenses/by/4.0/>)

reaction within direct ethanol fuel cells. It is also utilized in sensor platforms that rely on SERS (surface-enhanced Raman scattering) SPR (surface plasmon resonance), SEF (surface-enhanced fluorescence) and some other techniques [5-7]. Unfortunately, in these applications, the properties of the material are significantly influenced by factors such as the size and shape of grains, surface morphology, grain growth, as well as surface roughness [1,8]. In the case of SERS, the enhancement factor of the signal is directly related to the nanoscale morphology [9]. Additionally, the catalytic activity of metal nanostructures can be easily controlled by adjusting their shape [10]. Gold nanostructures with specific surface roughness and morphology have the potential to be used in various technological applications, including selective solar absorbers, antireflection coatings, and diffraction gratings [8].

The study of the morphology of thin films and understanding their growth mechanisms is crucial. It provides insights into how these films form and develop with variations in thickness [11]. This knowledge is essential for fabricating nanostructured materials in a controlled manner to achieve desired properties. These systems are considered fully functional materials because their chemical and physical properties, such as catalytic, electronic, optical, and mechanical properties, are strongly influenced by their structural characteristics, including size, shape, and crystallinity [11]. To manipulate the structural properties of these systems, innovative bottom-up procedures are being developed, moving away from traditional top-down scaling schemes. This allows for greater control over the fabrication process and opens up possibilities for tailored nanostructures with specific properties. As a result, there is a renewed interest in these studies, especially in the field of nanotechnology applications. The main focus of these studies is to gain a deep understanding of the kinetic growth mechanisms of thin films. By doing so, researchers can establish correlations between the observed structural changes and various process parameters. These parameters include deposition features like rate and time, as well as factors related to subsequent processes such as annealing temperatures and time, ion beam energy, and fluence. By studying how these process parameters affect the growth and structure of thin films, researchers can optimize and control the fabrication process to achieve desired properties and functionalities. This knowledge is crucial for advancing the field and developing innovative applications in areas such as nanotechnology.

Atomic force microscopy (AFM) is a very good technique for surface topography of thin films. It provides real space imaging and offers high spatial resolution, allowing researchers to examine the surface morphological characteristics in detail. Additionally, AFM can be used to quantitatively analyze the interface width using the dynamic scaling method. Several research groups [1, 8, 12-14] have been actively working on understanding surface roughness and growth mechanisms using AFM. This technique holds great potential for advancing our knowledge in various fields.

Fractal and multifractal concepts are indeed valuable tools for understanding the complexity of surface

morphology. While a fractal system can be described by a single scaling exponent, a multifractal system, which is a generalization of fractals, requires a continuous spectrum of exponents known as the singularity spectrum. This spectrum provides a more comprehensive description of the system's dynamics, as it varies depending on the position within the structure. The multifractal spectrum is particularly useful for identifying surface roughness and determining the shape of valleys and peaks in rough surfaces [14]. By analyzing the multifractal properties of a film surface, researchers can obtain more detailed information compared to traditional fractal analysis [15]. This information is crucial for understanding the relationship between the structure and properties of materials [16]. One of the advantages of multifractal analysis is its high precision, as it allows for a more accurate characterization of surface features. Additionally, it offers the benefit of low computation time and easy implementation, making it a popular choice in various studies. Overall, multifractal analysis plays a significant role in advancing our knowledge of surface morphology and its implications in different fields. However, it is important to acknowledge that the accuracy of multifractal analysis results can be influenced by various factors, such as data quality, methodology selection, and scale considerations. Researchers should approach multifractal analysis with a critical mindset, considering these factors to ensure the reliability and validity of their findings.

In this work, we focused on analyzing the surface morphology and conducting multifractal analysis of AFM images of Au films with different thicknesses, which were prepared using the electrodeposition technique. Our analysis revealed the presence of self-similar and multifractal characteristics in the morphology of the Au films. Additionally, we made an effort to investigate how these features are influenced by the thickness of the films. This research provides valuable insights into the relationship between film thickness and the self-similarity and multifractality of Au film surfaces.

2. Experimental

2.1. Material

In the process of preparing Au thin films, electrodeposition is used with a single electrolyte solution. The electrolyte consists of 0.080 mol/L $\text{Na}_3\text{Au}(\text{SO}_3)_2$ and 0.32 mol/L Na_2SO_3 . The electrodeposition takes place at room temperature. Substrate is silicon that was pre-coated with a gold seed layer (with surface rms roughness in the range of 3-4 nm).

2.2. Preparation of Au films

The electrochemical cell utilized a single compartment configuration, featuring a counter electrode made of Pt wire and a reference electrode of Ag/AgCl (saturated KCl). The working electrodes were cleaned Si with an area of 0.25 cm². The current density applied was 2 mA/cm². The solution's pH was maintained at 8. Throughout the electrodeposition experiments, the solution was stirred at a speed of 300 rpm. Cyclic voltammograms and electrodeposition were recorded using a computer-controlled EG&G potentiostat. Following modification, the

electrode underwent a thorough rinsing with distilled water, dried, and stored in air. All measurements were conducted after a comprehensive rinsing of the electrode.

2.3. Characterization

The polycrystalline structure of Au thin films was examined using X-ray diffraction using a Philips X'PERT-MRD diffractometer. Cu K α radiation with a wavelength of 0.15418 Å was utilized for the analysis. The surface morphologies of the films were investigated using an atomic force microscope (Bruker Nanoscope V) in tapping mode under atmospheric conditions. Surface morphology of thin films was measured by using AFM in the contact mode. High-quality etched silicon probes were employed for the AFM measurements. Scans were performed on a wide area of 1 × 1 μm² for each sample. The AFM provided height data with a resolution of 256 × 256 pixels. The reproducibility of the results was verified by imaging several regions of the same sample. The data analysis was performed with Gwyddion Software. In order to verify the AFM images, they were converted into ASCII type data.

3. Models and methods

3.1. Roughness

The roughness of the surface is quantified by the interface width, which is determined as the root mean square (RMS) of the height. In the case of an AFM image with dimensions M × N pixels, the two-dimensional RMS roughness can be calculated using the following formula [16]:

$$w = \sqrt{\frac{1}{MN} \sum_{i=1}^M \sum_{j=1}^N [z(i, j) - \langle z(i, j) \rangle]^2} \quad (1)$$

where $z(i, j)$ denotes the surface height measured by the AFM at point (i, j) , and $\langle z(i, j) \rangle$ represents the average given by:

$$\langle z(i, j) \rangle = \frac{1}{MN} \sum_{i=1}^M \sum_{j=1}^N z(i, j) \quad (2)$$

3.2. Multifractal analysis

The widely used multifractal analysis technique for characterizing surfaces is the spectrum of singularities $f(\alpha)$ multifractal method. This method involves the application of the box-counting method in multifractal analysis. In the box-counting method, an AFM image is divided into numerous boxes of size $\varepsilon \times \varepsilon$. The average film deposition probability in each box (i, j) is denoted as P_{ij} :

$$P_{ij}(\varepsilon) = \frac{h_{ij}}{\sum h_{ij}} \quad (3)$$

Where h_{ij} is the average height of the box (i, j) of size ε measured from the data planes which have similar depths for the Au deposited film and substrates, so that $\sum P_{ij} = 1$ [18]. For multifractal measures, the scaling relations for the box (i, j) at scale ε can be described as follows:

$$P_{ij} \propto \varepsilon^\alpha, N_\alpha(\varepsilon) \propto \varepsilon^{-f(\alpha)} \quad (4)$$

Here α is Lipschitz–Holder exponent and indicates singularity of the probability subsets. If all boxes exhibit a similar exponent α , it indicates monofractality. The quantity $N_\alpha(\varepsilon)$ represents the number of boxes with a size of ε that share the same α exponent. The function $f(\alpha)$ corresponds to the fractal dimension of the subset of the measure characterized by the α exponent, and it represents the singularity spectrum. By plotting $f(\alpha)$ against α , the multifractal spectrum is obtained, enabling a quantitative evaluation of the level of inhomogeneity in the reaction probability distribution. To calculate $f(\alpha)$, it is recommended to define a partition function as described in reference [15].

$$Z(q, \varepsilon) = \sum P_{ij}^q(\varepsilon) = \varepsilon^{\tau(q)} \quad (5)$$

where the exponent q , is a real parameter, called moment order and $\tau(q)$ is the correlation exponent or Mass exponent of order q . The variables $f(\alpha)$ and α are connected to $\tau(q)$ through a Legendre transform, as indicated by reference [19].

$$\alpha(q) = \frac{d\tau(q)}{dq} \quad (6)$$

$$f(\alpha) = q\alpha(q) - \tau(q) \quad (7)$$

Although the range of q is defined as $(-\infty < q < \infty)$, it is important to note that the values of q never actually reach infinity. This is because, for a specific and finite set of q values, both α and $f(\alpha)$ reach their saturation q values. The maximum value of q is determined by the distribution probability. The variation of $f(\alpha)$ in relation to α forms a continuous curve known as the multifractal spectrum.

4. Results and discussion

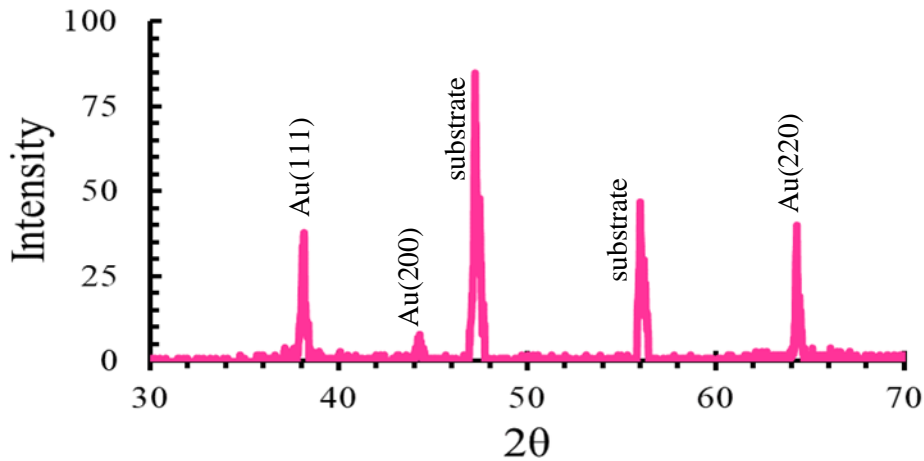
Fig. 1 displays an XRD pattern representing Au films with a thickness of 200 nm. The diffraction peaks observed at 2θ (h k l) values of 38.33 (1 1 1), 44.49 (2 0 0) and 64.61 (2 2 0) match those reported for standard gold metal (JCPDS card no. 04-0784). Therefore, Au deposits exhibit a face-centered cubic (FCC) phase. Notably, the dominant peak at (1 1 1) suggests that our electrodeposited Au films exhibit a (1 1 1)-textured polycrystalline structure. By employing the Scherrer equation [20]:

$$D = \frac{0.9\lambda}{\beta \cos \theta} \quad (8)$$

(λ is the X-ray wavelength, θ the diffraction angle, and β the width at half maximum (FWHM) of the respective XRD peak) and considering the width of the (1 1 1) peak, the average crystallite size is determined to be 25 nm.

Table 1. The multifractal spectra of the Au films.

Thickness	α_{min}°	α_{max}°	$\Delta\alpha^{\circ}$	$f(\alpha_{min}^{\circ})$	$f(\alpha_{max}^{\circ})$	Δf
200 nm	1.75	2.77	1.02	1.52	0.96	0.58
300 nm	1.71	2.88	1.17	1.52	0.93	0.59
400 nm	1.68	2.98	1.30	1.50	0.90	0.60

**Fig. 1.** XRD pattern of Au film prepared by electrodeposition with thickness of 200 nm.

In Figure 2, selected AFM images of Au films with varying thicknesses are presented. It is evident that the surfaces of the Au films consist of continuous island-like grains. These islands develop both vertically and laterally as the film thickness increases. The root mean square roughness values, calculated using equation (1), are 4.21 nm, 5.38 nm, and 7.71 nm for film thicknesses of 200 nm, 300 nm, and 400 nm, respectively. This clearly demonstrates that the roughness increases with the film thickness, indicating a strong influence of aggregation, structure, and grain size on the surface morphology. However, it is important to note that the roughness parameter alone does not provide a comprehensive description of the thin film surfaces. Local characteristics, traits, and specific details regarding the shape of peaks and valleys are not captured by these parameters. Additionally, it has been observed that roughness parameters based on conventional theories are dependent on the sampling interval of the measuring instrument [21].

In simple fractal analysis, the computation of $N(\epsilon)$ does not account for the recognition of height differences across different boxes. As a result, the slope of the $N(\epsilon)$ versus ϵ curve in logarithmic scale tends to resemble that obtained in two dimensions at larger ϵ values. However, this limitation can be overcome by employing multifractal analysis, which provides a more comprehensive understanding of the data. In this particular study, multifractal analysis has been conducted on AFM images. This involved identifying profiles and calculating the singularity spectrum, which determines the distribution of roughness exponents across the entire range. In multifractal analysis, the presence of linearity in the logarithmic scale graph of $Z(q, \epsilon)$ versus ϵ is considered significant. This linear region is referred to as the scaling

region. In an ideal regular multifractal, linearity is observed across all moments of q . However, in some cases, this linearity can approach zero or even extend to infinity. On the other hand, a random multifractal tends to exhibit a preferable linearity between $\ln Z(q, \epsilon)$ and $\ln \epsilon$.

In our image analysis, we initially investigate the scaling region. We calculate the partition function $Z(q, \epsilon)$ for various values of q and plot it against different box sizes in Figure 3. The plot demonstrates the linearity of $\log(Z)$ in relation to $\log(L)$. The range of q values considered is from -5 to 5, while the box sizes (ϵ) are chosen as 1/256, 1/128, 1/64, 1/32, 1/16, 1/8, 1/4, 1/2, and 1. It is evident that the $\ln Z(q, \epsilon)$ vs $\ln \epsilon$ graph (scaling region) exhibits good linearity for all q -moments and box sizes of ϵ . Although the results are not presented here, we have verified the $\ln Z(q, \epsilon)$ vs $\ln \epsilon$ graphs for other Au films using the same method. Consequently, multifractal analysis can be effectively employed to quantitatively characterize the electrodeposited Au films. This scaling enables one to calculate the mass exponent $\tau(q)$ for moment orders within the range of $-5 < q < 5$ with a step size of 0.2, utilizing equation (5) in two dimensions. Figure 4 illustrates $\tau(q)$ as a function of q for film surfaces with varying thickness. It is evident that $\tau(q)$ exhibits nonlinearity with respect to q , indicating the multifractal nature of the studied surfaces. It is important to note that the estimation of $\tau(q)$ is less statistically significant for larger values of q due to the small size of the available data.

Equations (6) and (7) are used to calculate the parameters of the multifractal spectrum for the samples. The obtained results are presented in Table 1. These parameters play a crucial role in describing the multifractal nature of the samples. Figure 5 illustrates that $f(\alpha)$ exhibits continuous variations as a function of α for each film

thickness. The width and shape of the $f(\alpha)$ spectrum differ for each sample. Notably, the multifractal spectra display a hook-like shape with the tip pointing towards the left. Furthermore, it is observed that the singularity spectrum becomes broader as the film thickness increases, indicating greater irregularity in thicker surfaces. Similar findings have been reported in studies on the morphology of different film surfaces with varying thickness [1, 16, 21, 22].

The singularity strengths, represented by the maximum (α_{max}) and minimum (α_{min}) values, are associated with the zone of sets where the measurements have been conducted, as mentioned in reference [21]. The values of $f(\alpha_{max})$ and $f(\alpha_{min})$ correspond to the fractal dimension of two regions. Table 2 provides the multifractal spectra parameters for the Au films. It is observed that α_{max} increases while α_{min} decreases with increasing film thickness. The width of the multifractal spectrum, $\Delta\alpha$, which is defined as the range of height probability distribution, appears to become narrower as the film thickness decreases. The magnitude of $\Delta\alpha$ is indicative of the strength of multifractality, with smaller (greater) $\Delta\alpha$ associated with weaker (stronger) multifractality. The thickness of the film strongly influences the value of $\Delta\alpha$, as it increases with increasing film thickness, resulting in a rough and irregular film surface and a more nonuniform height probability.

In multifractal formalism, as ε goes to zero, α_{min} and the maximum height probability P_{max} , are related as $P_{max} = \varepsilon^{\alpha_{min}}$. Similarly, there is a corresponding relation between α_{max} and P_{min} , which is given by ($P_{min} = \varepsilon^{\alpha_{max}}$).

Thus, $\Delta\alpha$ is used to determine the range of probabilities, where $P_{max}/P_{min} = \varepsilon^{-\Delta\alpha}$. The function $f(\alpha_{max})$ represents the number of boxes with a minimum height probability, denoted as $N_{P_{min}(\varepsilon)}$, which can be approximated as $N_{\alpha_{max}(\varepsilon)} \sim \varepsilon^{-f(\alpha_{max})}$. Similarly, $f(\alpha_{min})$ represents the

number of boxes with the maximum height probability, denoted as $N_{P_{max}(\varepsilon)}$, which can be approximated as $N_{\alpha_{min}(\varepsilon)} \sim \varepsilon^{-f(\alpha_{min})}$ [15]. The height interval of the multifractal spectrum, denoted as Δf , represents the difference between the values of $f(\alpha_{min})$ and $f(\alpha_{max})$. This difference can be utilized to describe the ratio of the number of boxes with maximum probabilities ($N_{P_{max}}$) to the number of boxes with minimum probabilities ($N_{P_{min}}$). This ratio can be expressed as $N_{P_{max}}/N_{P_{min}} = \varepsilon^{-\Delta f}$. Additionally, Δf is also defined as the height interval of the multifractal spectrum.

The given information suggests that when Δf is greater than zero, it implies that the probability of finding the deposit at the highest regions is much larger than at the lowest regions. In the case of electrodeposited Au films, all values of Δf obtained were positive, which is consistent with a left hook-like shape of the spectra.

Additionally, the ratio $N_{P_{max}}/N_{P_{min}}$ for an Au film with a thickness of 200 nm, at $\varepsilon = 1/256$, was found to be 67.49. This ratio decreases as the film thickness increases. It should be noted that this quantitative description cannot be obtained using conventional statistical treatments.

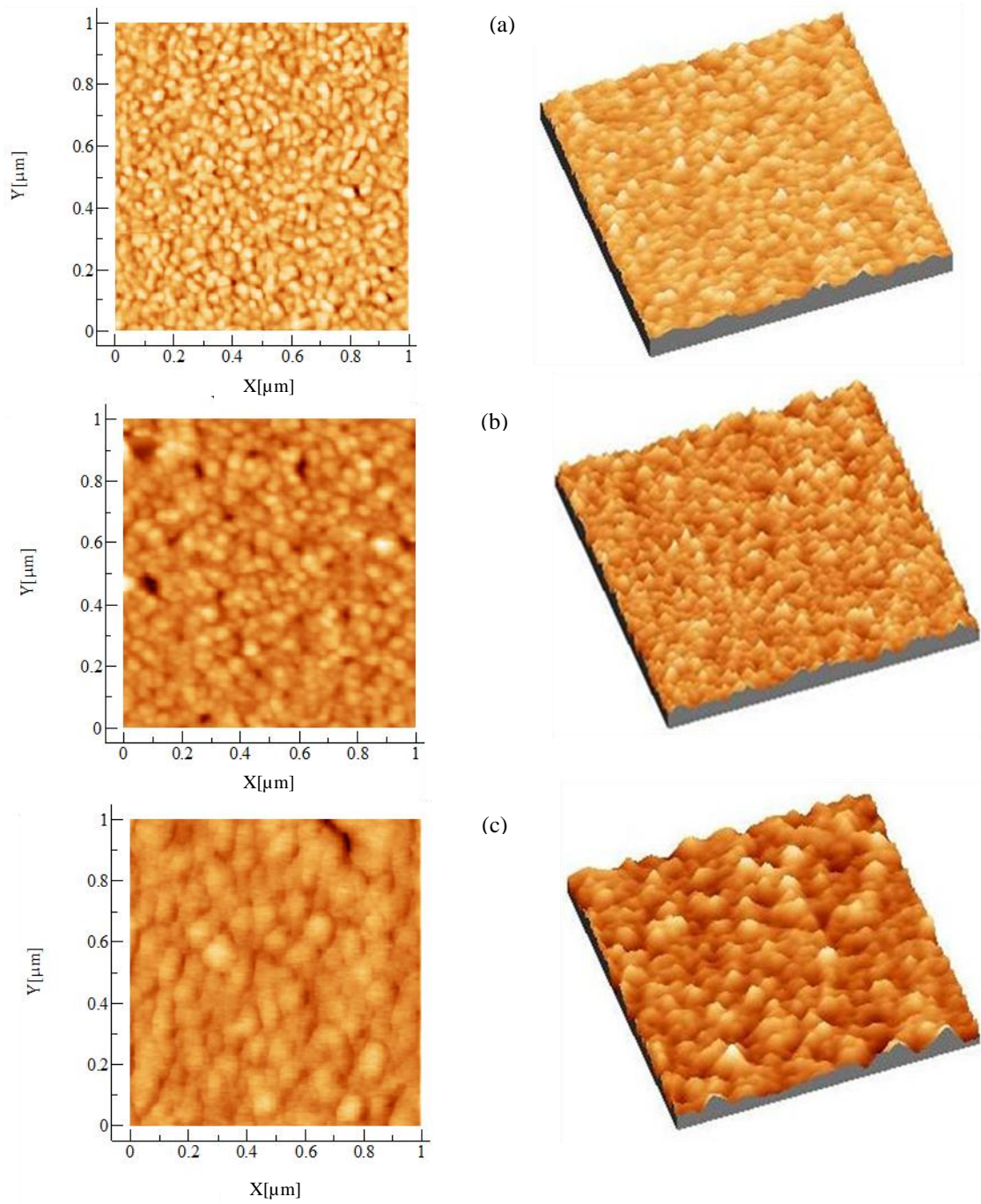


Fig. 2. Selective 2D and 3D AFM images of electrodeposited Au films with thicknesses of a) 200 nm, b) 300 nm, and c) 400 nm.

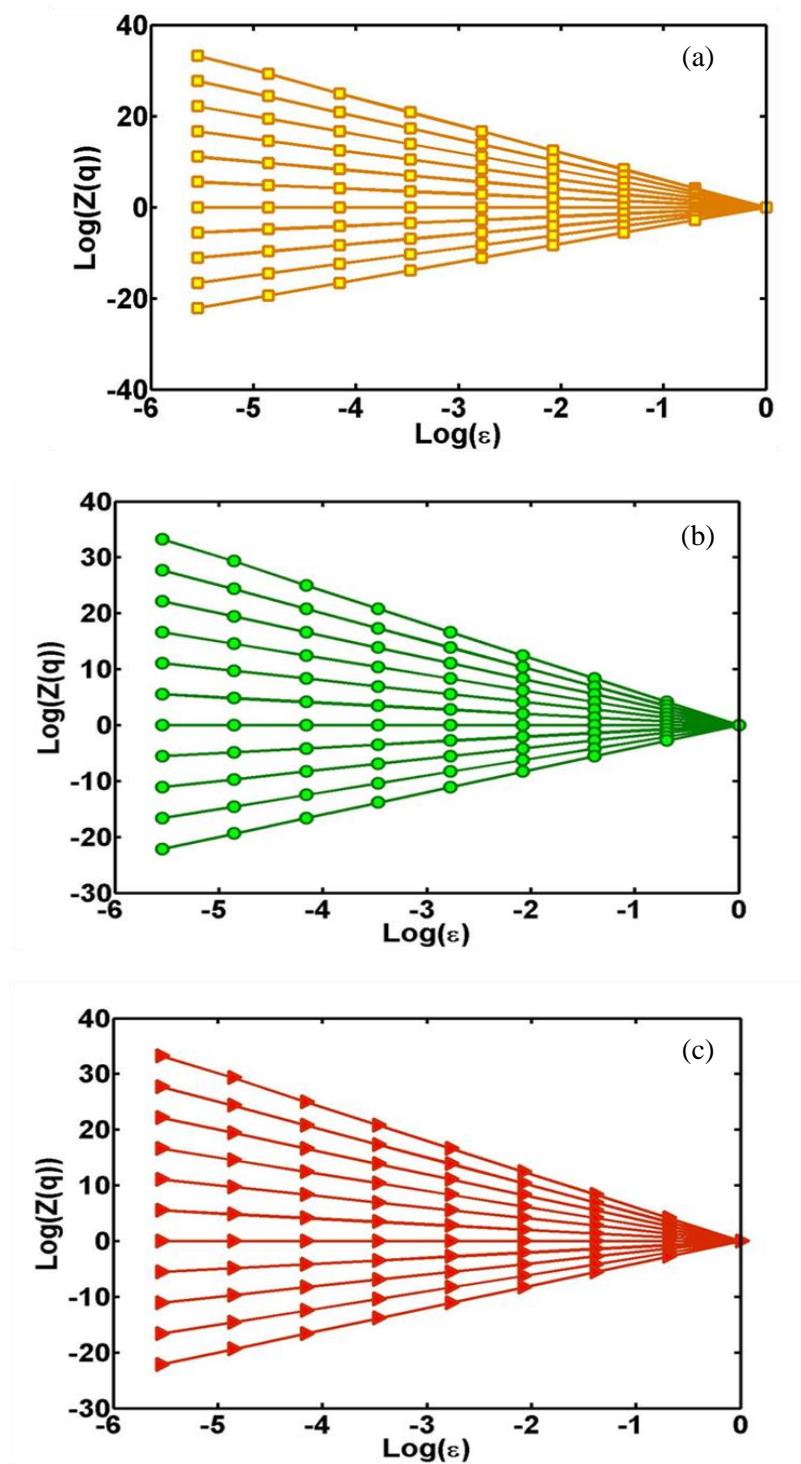


Fig. 3. Plots of $\ln Z(q, \epsilon)$ vs $\ln \epsilon$ for different values of q for Au films with thicknesses of a) 200 nm, b) 300 nm, and c) 400 nm.

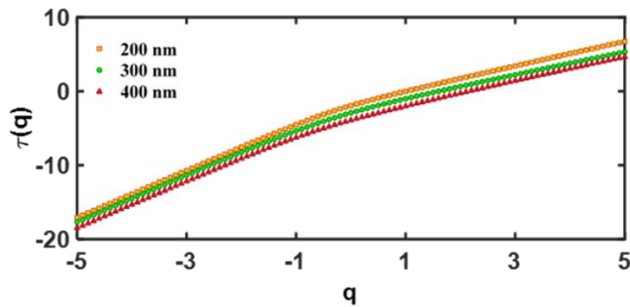


Fig. 4. Plot of $\tau(q)$ as a function of q for Au film surfaces with different thicknesses.

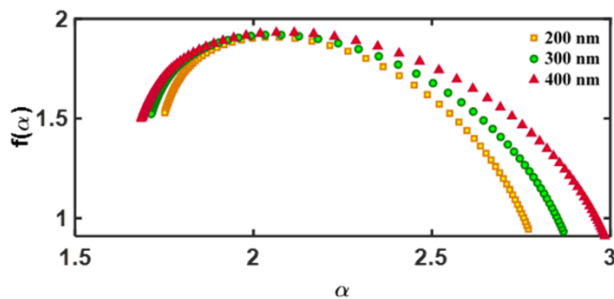


Fig. 5. $f(\alpha)$ versus α for Au film surfaces with different thicknesses.

5. Conclusion

In this study, we examined the surface morphology of gold thin films produced using the electrodeposition method. We used atomic force microscopy (AFM) to analyze the surface morphology and employed interface width and multifractal analysis to characterize these films. The AFM images clearly revealed that the roughness of the surface increased as the film thickness increased. However, using conventional parameters such as roughness (w) alone was insufficient to provide a complete description and reveal local details of the surface morphology. Therefore, we performed a two-dimensional multifractal analysis. The multifractal analysis demonstrated that the film surfaces exhibited a multifractal nature. The parameters of the multifractal spectra were used to characterize the growth and interface width of the thin films. The multifractal analysis proved to be more informative compared to conventional methods. Our findings showed that the width of the multifractal spectrum ($\Delta\alpha$), which indicates the strength of multifractality, increased with film thickness. The difference in height intervals of the multifractal spectrum (Δf) could determine the ratio of the number of low and high regions of the local details, thus describing the shape of valleys and peaks in various rough surfaces. It appeared that the nonuniformity of the height distribution increased with increasing thickness. Overall, our results indicate that multifractal analysis is capable of providing more detailed and reliable information compared to conventional methods.

Acknowledgements

The authors gratefully acknowledge the support of technical and vocational university.

Conflicts of Interest

The author declares that there is no conflict of interest regarding the publication of this article.

References

- [1] Yadav, R.P., Dwivedi, S., Mittal, A.K., Kumar, M. and Pandey, A.C., 2012. Fractal and multifractal analysis of LiF thin film surface. *Applied Surface Science*, 261, pp.547-553.
- [2] Noel, J.G., 2016. Review of the properties of gold material for MEMS membrane applications. *IET Circuits, Devices & Systems*, 10(2), pp.156-161.
- [3] Ayoub, S. and Beaulieu, L.Y., 2013. The surface morphology of thin Au films deposited on Si (001) substrates by sputter deposition. *Thin solid films*, 534, pp.54-61.
- [4] Gaur, S.P., Kothari, P., Maninder, K., Kumar, P., Rangra, K. and Kumar, D., 2017. Development and integration of near atmospheric N₂ ambient sputtered Au thin film for enhanced infrared absorption. *Infrared Physics & Technology*, 82, pp.154-160.
- [5] Cao, X., Peng, D., Wu, C., He, Y., Li, C., Zhang, B., Han, C., Wu, J., Liu, Z. and Huang, Y., 2021. Flexible Au micro-array electrode with atomic-scale Au thin film for enhanced ethanol oxidation reaction. *Nano Research*, 14, pp.311-319.
- [6] Chen, P.J. and Hsueh, C.H., 2021. Imprintable Au-based thin-film metallic glasses with different crystallinities for surface-enhanced Raman scattering. *The Journal of Physical Chemistry C*, 125(43), pp.23983-23990.
- [7] Lequeux, M., Mele, D., Venugopalan, P., Gillibert, R., Boujday, S., Knoll, W., Dostalek, J. and Lamy de la Chapelle, M., 2020. Plasmonic properties of gold nanostructures on gold film. *Plasmonics*, 15, pp.1653-1660.
- [8] Elias, J., Gizowska, M., Brodard, P., Widmer, R., Dehazan, Y., Graule, T., Michler, J. and Philippe, L., 2012. Electrodeposition of gold thin films with controlled morphologies and their applications in electrocatalysis and SERS. *Nanotechnology*, 23(25), p.255705.
- [9] Bechelany, M., Brodard, P., Elias, J., Brioude, A., Michler, J. and Philippe, L., 2010. Simple synthetic route for SERS-active gold nanoparticles substrate with controlled shape and organization. *Langmuir*, 26(17), pp.14364-14371.
- [10] Bond, G.C. and Thompson, D.T., 1999. Catalysis by gold. *Catalysis Reviews*, 41(3-4), pp.319-388.
- [11] Ruffino, F., Grimaldi, M.G., Giannazzo, F., Roccaforte, F. and Raineri, V., 2009. Atomic force microscopy study of the kinetic roughening in nanostructured gold films on SiO₂. *Nanoscale research letters*, 4, pp.262-268.
- [12] Ruffino, F. and Grimaldi, M.G., 2018. Morphological characteristics of Au films deposited on Ti: a combined SEM-AFM study. *Coatings*, 8(4), p.121.
- [13] Nasehnejad, M. and Nabiyouni, G., 2019. Studying magnetic properties and surface roughness evolution of Ag-Co electrodeposited films. *Journal of Magnetism and Magnetic Materials*, 490, p.165501.

- [14] Wadullah, H.M., Ali, M.H. and Abdulrazzaq, T.K., 2022. Structure, characteristics and corrosion behaviour of gold nanocoating thin film for biomedical applications. *Materials Research*, 25, p.e20210526.
- [15] Sun, X., Fu, Z. and Wu, Z., 2002. Fractal processing of AFM images of rough ZnO films. *Materials Characterization*, 48(2-3), pp.169-175.
- [16] Nasehnejad, M., Shahraki, M.G. and Nabiyouni, G., 2016. Atomic force microscopy study, kinetic roughening and multifractal analysis of electrodeposited silver films. *Applied Surface Science*, 389, pp.735-741.
- [17] Zhang, Y.H., Bai, B.F., Chen, J.B., Shen, C.Y. and Li, J.Q., 2010. Multifractal analysis of fracture morphology of poly (ethylene-co-vinyl acetate)/carbon black conductive composite. *Applied Surface Science*, 256(23), pp.7151-7155.
- [18] Chen, Z.W., Lai, J.K.L. and Shek, C.H., 2005. Multifractal spectra of scanning electron microscope images of SnO₂ thin films prepared by pulsed laser deposition. *Physics Letters A*, 345(1-3), pp.218-223.
- [19] Chaudhari, A., Yan, C.C.S. and Lee, S.L., 2003. Multifractal scaling analysis of autopoisoning reactions over a rough surface. *Journal of Physics A: Mathematical and General*, 36(13), p.3757.
- [20] Suryanarayana, C., Norton, M. G., 1999, X-ray diffraction, New York, Plenum Press.
- [21] Yadav, R.P., Singh, U.B., Mittal, A.K. and Dwivedi, S., 2014. Investigating the nanostructured gold thin films using the multifractal analysis. *Applied Physics A*, 117, pp.2159-2166.
- [22] Wang, W., Li, A., Zhang, X. and Yin, Y., 2011. Multifractality analysis of crack images from indirect thermal drying of thin-film dewatered sludge. *Physica A: Statistical Mechanics and its Applications*, 390(14), pp.2678-2685.